Consolidation of B4C–VB2 eutectic ceramics by spark plasma sintering

Demirskyi, Dmytro; Sakka, Yoshio; Vasylkiv, Oleg

2015

Demirskyi, D., Sakka, Y., & Vasylkiv, O. (2015). Consolidation of B4C–VB2 eutectic ceramics by spark plasma sintering. Journal of the Ceramic Society of Japan, 123(1443), 1051-1054.

https://hdl.handle.net/10356/83817

https://doi.org/10.2109/jcersj2.123.1051

Journal of the Ceramic Society of Japan 123 [11] 1051-1054 2015 Note

Consolidation of B_4C–VB_2 eutectic ceramics by spark plasma sintering

Dmytro DEMIRSKYI,[*,,†,‡] Yoshio SAKKA[*] and Oleg VASYLKIV[*,**]**

[*]National Institute for Materials Science, 1–2–1 Sengen, Tsukuba, Ibaraki 305–0047, Japan
[**]Nanyang Technological University, 50 Nanyang Avenue, 639798, Singapore

The in situ synthesis and consolidation of B_4C–VB_2 eutectic composites by spark plasma sintering (SPS) is reported. The microstructure properties were determined for composites with the B_4C–VB_2 eutectic composition as functions of the VB_2 content and the VB_2–VB_2 interlamellar spacing. A change of VB_2 concentration from 45 to 48 mol.% resulted in the formation of the rod-like eutectic microstructure. Indentation fracture toughness values higher than 4 MPa·m$^{1/2}$ were identified for eutectic composites with interlamellar spacings between 0.9 and 1.2 μm. The composites obtained by SPS with a composition of 45 mol.% VB_2 exhibited a lower Vickers hardness (23–24 GPa) and higher indentation fracture toughness (up to 4.5 MPa·m$^{1/2}$) than the eutectic composites with 48 mol.% of VB_2.

Key-words : Spark plasma sintering, Boron carbide, Eutectic, Toughness, Hardness

[Received May 21, 2015; Accepted August 23, 2015]

1. Introduction

Composites of transition-metal diborides embedded in a boron carbide matrix that exhibit good hardness and strength are considered attractive materials for high-temperature applications.[1)–6)] Since it is generally predicted[5)] that materials containing up to 30 vol.% of borides should have elevated crack resistance and high temperature strength. Higher boride content leads to spontaneous cracking, especially in non-eutectic composites, hence it is generally accepted that a composition close to the eutectic is optimal for consolidation.

Among such systems, B_4C–Me^VB_2 eutectic composites have not been studied as extensively as the B_4C–TiB_2 eutectic[1)–4)] and non-eutectic composites.[7),8)] In particular, B_4C–VB_2 remains largely unexplored among transition metal diboride composites with boron carbide owing to its high eutectic temperature (>2150°C). Single crystal vanadium diboride (VB_2) has a low specific-weight (5.1 g/cm^3), good wear resistance and electrical conductivity, and small hardness anisotropy.[9)] Furthermore, vanadium boride, in analogy with TiB_2, has a thermal expansion coefficient that differs most from that of boron carbide[5)] and, consequently, an increase in the fracture toughness is anticipated if the proper composite design is developed. Mizutani et al.[10)] showed that, for case of particulate composites of SiC–20 mol.% MeB_2, ceramic composites with VB_2 exhibited the highest toughness. In addition, Tanaka et al.[11)] showed that the small addition of VB_2 (5 vol.%) to SiC also resulted a high fracture toughness of 4.6 MPa·m$^{1/2}$.

Recent studies by Demirskyi et al.[12),13)] on B_4C–NbB_2 ceramics showed an alternative route for preparing high temperature ceramic composites with eutectic structures in situ by spark plasma sintering (SPS).[14)–18)] This method provides a new opportunity for studying non-oxide eutectic composites using the pressure during SPS as a controlling parameter. Namely, the pressure in SPS can be used to control the eutectic microstructure and to slightly decrease the eutectic temperature. SPS allows in situ synthesis of eutectic composites with melting points exceeding 2000°C, which allows some difficult to prepare composites, such as B_4C–VB_2, to be manufactured using unmodified SPS hardware.

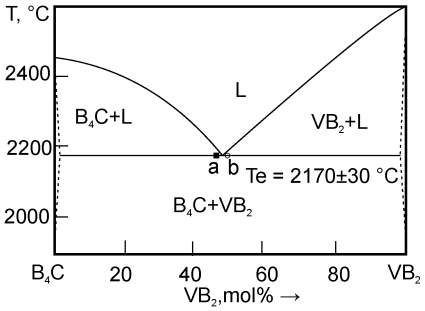

Fig. 1. Equilibrium phase diagram of the B_4C–VB_2 system,[7)] where (a) and (b) correspond to the structures of ceramic composites (Fig. 2) with 45 and 48 mol % VB_2 after SPS at 2150°C, respectively.

The work presented here extends a previous investigation of the B_4C–NbB_2 system[12),13)] and focuses on the B_4C–VB_2 system. The consolidation of eutectic composites near the eutectic point (**Fig. 1**) are explored using two limit values for the eutectic composition suggested by an earlier study by Ordan'yan et al.[6)] In addition, evaluation of the microstructural properties of B_4C–VB_2 ceramic eutectic composites prepared in situ by SPS is a presented.

2. Materials and methods

Commercially available VB_2 (−325 mesh, dav = 2–8 μm, American Elements, USA) and B_4C (dav = 1.5–5.0 μm, B_2O_3 < 0.75 wt.%, Cfree < 2 wt %, Sinopharm Chemical Reagent Co. Ltd., Singapore) powders were used as starting materials. Powder

† Corresponding author: D. Demirskyi; E-mail: dmytro.demirskyi@ntu.edu.sg, demirskyi.dmytro@nims.go.jp
‡ Present address: Nanyang Technological University, 50 Nanyang Avenue, 639798 Singapore

DOI http://dx.doi.org/10.2109/jcersj2.123.1051

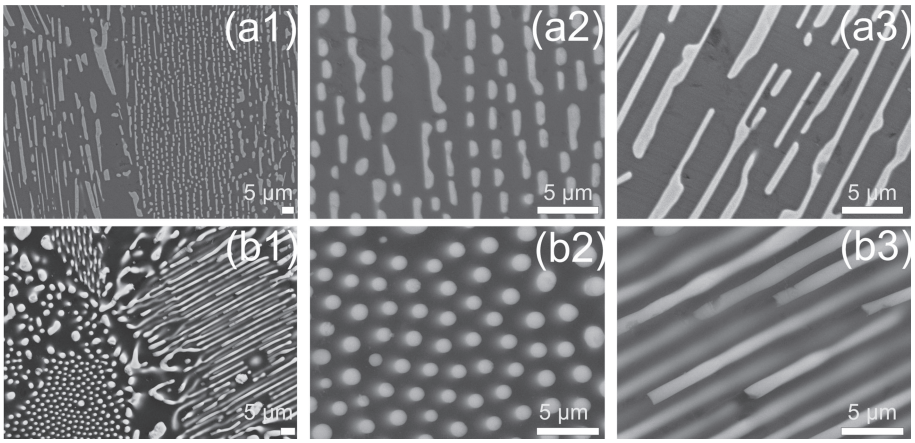

Fig. 2. Typical structures of B_4C–VB_2 eutectic composites with (a) 45 and (b) 48 mol.% VB_2 after SPS at 2150°C.

mixtures of B_4C and 45 and 48 mol.% VB_2 were prepared by wet-chemical mixing in alcohol followed by drying at about 100°C. The resultant powder was screened through a 60-mesh screen.

The SPS experiments were performed using the 'Dr. Sinter' apparatus (Sumitomo, Japan). Initially, a pressure of 20 MPa was applied to ensure sufficient electrical contact between the powder tablet and the graphite die. The pressure was then increased to 60 MPa and the temperature was increased to 800°C. A dwell time of 1 min at 800°C was used to focus a pyrometer on the outer die wall surface. Then the temperature was increased at a heating rate of 100°C·min^{-1} up to a sintering temperature of 1800°C with a dwell time of 1 min. This was followed by rapid heating (250°C·min^{-1}) to a temperature of 2150°C. To avoid the collapse of the sample due to liquid eutectic formation, the pressure was manually decreased from 60 to 15 MPa at temperatures between 2000 and 2050°C.[12),13)] SPS was performed in an argon gas medium with a flow rate of 2 l·min^{-1}.

After SPS consolidation, specimens were first ground with SiC paper to form a flat surface, followed by grinding with diamond disks to a 0.5 μm finish. Microstructural observations and analyses were carried out on the polished samples using a Hitachi SU 8000 cold-emission field emission scanning electron microscope (SEM).

Hardness was determined by an MMT-7 Vickers hardness tester (Matsuzawa MMT-7; Matsuzawa SEIKI Co., Ltd., Tokyo, Japan), using loads ranging from 0.98 to 19.6 N with a dwell time of 15 s following the standard procedure (ASTM C 1327-15). The fracture toughness was calculated using the half length of the crack radius (c) formed around the corners of indentations at loads (L) of 4.8–19.6 N using the equation $K_{IC} = 0.073\ (L/c^{3/2})$.[19),20)] The hardness and fracture toughness for 20 points were averaged.

3. Results and discussion

The phase diagram of B_4C–VB_2 is presented in Fig. 1, where the melting point for the eutectic composition with 45–48 mol.% is 2170 ± 30°C[6)]. In the present investigation two limit values (i.e. 45 and 48 mol.% VB_2) of the eutectic composition and a consolidation temperature of 2150°C were selected.

The typical microstructure of the eutectic composites with 45 and 48 mol.% VB_2 are presented in **Fig. 2** [(a) and (b), respectively]. Since all samples were consolidated under the same conditions, it is clear that with increasing VB_2 content the shape of the diboride eutectic inclusions becomes more round and corresponds to a typical rod-like structure. A slight increase in rod size, compared to the 45 mol.% VB_2 eutectic, is also visible.

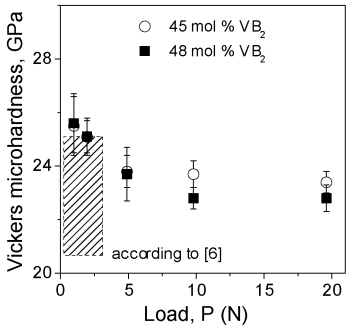

Fig. 3. Effect of load on Vickers hardness of B_4C–VB_2 eutectic composites prepared by in situ SPS consolidation. Symbols for each composition have the same meaning as that in Fig. 1.

All specimens prepared during this study had almost full density. Some minor porosity was visible during examination of polished specimens by optical microscopy – it was introduced during polishing of composites, i.e. due to removal of VB_2 inclusions. Anyway, we believe that application of the moderate pressure during cooling of the eutectic composite ensured enclosure of pores associated with melting of the ceramic composite.

According to **Fig. 3**, the composites with the eutectic composition exhibited microhardnesses (24–26 GPa) similar to those previously reported.[6)] A further increase in the load (9.8 N, Hv9.8) resulted in a slight decrease in hardness to 22.8–24.3 GPa, followed by a further decrease to 23.5 ± 0.4 GPa at a 19.6 N load. This trend is typical for brittle ceramics and was previously reported by White and Dickey for the eutectic ceramic of B_4C–TiB_2.[21)]

A decrease in interlamellar spacing (λ) was found with the decrease in hardness (Hv9.8) of the eutectic composite with 45 and 48 mol. % VB_2. A maximum in hardness for both composites was found. In case of 45 mol.% VB_2 the maximum was observed for $\lambda = 1.1$ μm with values of 23.7 ± 0.3 GPa. For the 48 mol.% VB_2 the maxim hardness of 23.5 ± 0.5 GPa corresponded to $\lambda = 1.3$ μm (**Table 1**). In the case of the 48 mol.% VB_2 specimens, a maximum in fracture toughness (4.2 ± 0.5 MPa·m$^{1/2}$) was also observed around $\lambda = 1$ to 1.1 μm. For the case of the 45 mol.% VB_2, the increase in λ from 0.8 to 1.1 μm resulted in the decrease of K_{IC} from 4.3 ± 0.2 to 3.9 ± 0.5 MPa·m$^{1/2}$. We also noted that a mean half length of the crack radius, $c = a + l$, where a is the indent diagonal and l is the mean crack length from the indent's corner, increase steadily with load applied during the indentation test. In 45 mol.% VB_2 ceramic composites with $\lambda = 0.8$ μm, mean

Table 1. Microstructural characteristics and properties of B_4C–VB_2 ceramics

VB_2 content, mol.%	λ, μm	Diameter of eutectic inclusions, d, μm	Hv0.98*, GPa	Hv9.8, GPa	K_{IC}, MPa·m$^{1/2}$
45	0.8 ± 0.13	1.1–1.5	25.5 ± 0.8	21.7 ± 0.6	4.3 ± 0.2
45	1.1 ± 0.15	1.2 ± 0.15	25.8 ± 0.7	23.7 ± 0.3	4.2 ± 0.5
45	1.3 ± 0.15	1.2 ± 0.2	25.4 ± 0.7	22.5 ± 0.7	3.9 ± 0.5
48	0.8 ± 0.12	1.4 ± 0.2	25.6 ± 1.1	22.1 ± 0.6	3.6 ± 0.2
48	1.0 ± 0.1	1.4–1.9	26.1 ± 0.7	22.3 ± 0.3	4.2 ± 0.5
48	1.1 ± 0.12	1.4–1.9	26.6 ± 0.9	23.2 ± 0.3	4.1 ± 0.5
48	1.3 ± 0.1	1.3–1.8	25.7 ± 0.8	23.5 ± 0.5	3.5 ± 0.4
35 NbB_2[12]	1.2 ± 0.17	1.1 ± 0.1	32.3 ± 1.1	26.3 ± 1.1	5.2 ± 0.6
25 TiB_2[3]	2.0	—	~40**	—	5.6**
25 TiB_2[1]	1–2	—	—	25.6	4.5
25 TiB_2[4]	1.9		~34	26.32 ± 1.11	2.47 ± 0.30
8.15 vol.% VB_2[5]	—	—	23.8	—	—
13.6 vol.% VB_2[5]	—	—	26.0	—	—
VB_2[27]	—	—	27.46 ± 0.12**	—	—
B_4C[25]	—	—	—	31.31 ± 0.79	2.84 ± 0.11
B_4C[26]	—	—	—	22.51	2.21

Notes: *load of 0.98 N was used. **load of 1.96 N was used.

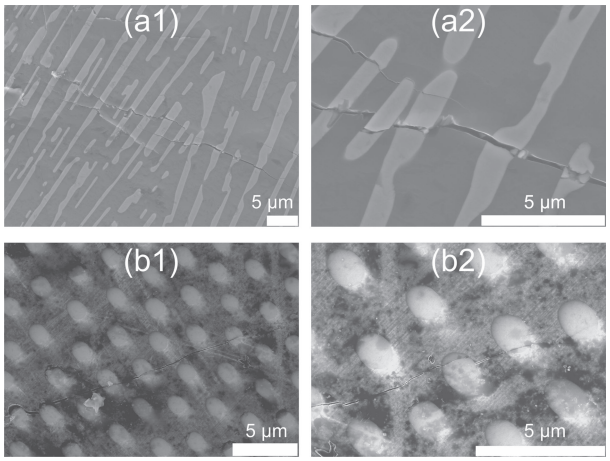

Fig. 4. Crack propagation in B_4C–VB_2 ceramic composites after indentation with a load of 19.6 and 9.8 N: (a) 45 and (b) 48 mol.% VB_2.

values of the c at increased from 16.25 ± 1.35 to 30.35 ± 2.55 and 53.8 ± 1.7 μm at loads of 4.9, 9.8 and 19.6 N, respectively.

Figure 4 shows the typical crack propagation observed after Vickers indentation for the (a) 45 and (b) 48 mol.% VB_2 eutectic composite after applying a (a) 19.6 and (b) 9.8 N loads. In both cases indentation surface was perpendicular to the pressure applied during SPS. The crack propagation path was both intergranular and intragranular. Transgranular fracture and crack branching were major mechanisms contributing to good fracture toughness in the case of the 45 mol.% VB_2 composites. Fibrils of material deforming between crack faces was also observed [Fig. 4(a2)]. Moreover, portions of the materials were observed to bridge across crack wakes. These results suggested that the interface bonding strength between VB_2 and B_4C was higher than that usually observed for sintered composites. Furthermore, in the case of the 48 mol.% VB_2 composites, crack bridging and crack deflection were the main toughening mechanisms. This suggests that the slightly higher fracture toughness in case of 45 mol.% VB_2 composites is due to the operation of different toughening mechanisms.

As mentioned in introduction, coefficients of thermal expansion (CTE) between vanadium diboride reinforcements differs most from that of boron carbide matrix (8.1×10^{-6} and 5.6×10^{-6} K^{-1}, respectively).[5] Therefore, thermal residual stresses in composites naturally arise owing to the coupling of different phases with different thermo-elastic properties. The magnitude of the residual stresses depends on the difference of elastic properties and CTE between phases multiplied by the temperature difference at which elastic stresses develop (ΔT). The proper evaluation of these tensile stresses in the matrix becomes particularly important when high temperature composites are considered, since ΔT for these types of composites is high enough to generate residual stresses in the order of the tensile strength of matrix itself. Measurements of residual stresses performed by Raman spectroscopy and X-ray diffraction in ZrB_2–SiC composites[22] and pointed out that stresses begin to accumulate at ~1400°C during cooling from the processing temperature.

The result is a tensile stress state in the matrix σ_m and a corresponding compressive stress state in the reinforcing phases, σ_r, was calculated with Taya et al.'s model:[23]

$$\sigma_m = E_m \frac{2f\beta\varepsilon^*}{A} \quad (1)$$

and

$$\sigma_r = -\frac{(1-f)\varepsilon^*}{f}\sigma_m \quad (2)$$

$$A = (1-f)(\beta+2)(1+\nu_m) + 3\beta f(1-\nu_m) \quad (3)$$

where f is the reinforcement volumetric fraction (0.35 in case of 45 mol.% VB_2) and

$$\beta = \frac{1+\nu_m}{1-2\nu_r}\frac{E_r}{E_m} \quad (4)$$

E_r, E_m, ν_r and ν_m are Young's modulus and Poisson ratio of reinforcement and matrix, respectively, and ε^* is the thermal expansion misfit strain:

$$\varepsilon^* = (\alpha_r - \alpha_m)\Delta T \quad (5)$$

where α_r, α_m the thermal expansion coefficients of reinforcement and matrix, respectively, and ΔT is the temperature at which stresses begin to accumulate, preset as 1400°C.[22]

Upon cooling the composite, the VB_2 phase is found to be in tension and the B_4C matrix is found to be in compression, which is expected as CTE of VB_2 is larger than the CTE of B_4C. As

result, the B_4C matrix is under residual compressive stress of $\sigma_m = 600$ MPa, and $\sigma_r = -5.63$ MPa at reinforcement.

These large residual compressive stresses developed in matrix may lead to a substantial increase in fracture toughness. Similar situation was observed in TaC-based[24] ceramics and lead to reasonable increase in fracture toughness from 3.66 to 4.7 MPa $m^{1/2}$. Furthermore, according to the Taya's[23] model, using a d of 1.1 μm, the stress intensity factor, ΔK_I, can be evaluated as 2.28 and 2.34 MPa $m^{1/2}$, in the case of 45 and 48 mol.% VB_2–B_4C eutectic composites, respectively. However, these values are not connected with the specific eutectic microstructure, and hence a further testing is needed by comparing composites with similar composition and the eutectic and non-eutectic structures.

In general, the fracture toughness of the eutectic composites was higher, or similar to, the values reported for monolithic B_4C (2–4 MPa·$m^{1/2}$)[25),26] and other eutectic composites with boron carbide (Table 1).[27] This illustrates that a boron carbide matrix limits the fracture toughness of B_4C–VB_2 eutectic composites, the while chemical composition of VB_2 inclusions controls the hardness. This suggests that a further increase in the toughness of lightweight eutectic composites of B_4C–Me^VB_2 may be achieved by either the formation of a $Me^{IV}Me^VB_2$ solid solution, or by changing a matrix to silicon carbide.

4. Summary

B_4C–VB_2 ceramic composites were produced by high-temperature spark plasma sintering (2150°C) via in situ formation of eutectic grains during the consolidation process. Uniform eutectic composites with a rod-like structure and wide interlamellar spacing (λ) were prepared. Microstructures close to the perfect rod-like eutectic structure were identified for the case of 48 mol.% VB_2 composites. Formation of such a structure contributed to a moderate fracture toughness (~4 MPa·$m^{1/2}$) with crack bridging and crack deflection being the main toughening mechanisms. In the case of the 45 mol.% composite, crack branching and transgranullar fracture contributed to the K_{IC} of 3.9–4.3 MPa $m^{1/2}$. In spite of the microstructure difference, eutectic composites with 45 and 48 mol.% VB_2 had similar hardness values of 21.7–23.5 GPa.

Acknowledgments This study was conducted with financial support from a JSPS Postdoctoral Fellowship by the Japan Society for the Promotion of Science. This work was partially supported by Grant-in-Aid for Scientific Research B from Japan Society for the Promotion of Science (JSPS).

References

1) I. Bogomol, H. Borodianska, T. Zhao, T. Nishimura, Y. Sakka, P. Loboda and O. Vasylkiv, *Scr. Mater.*, 71, 17–20 (2014).
2) I. Bogomol, T. Nishimura, O. Vasylkiv, Y. Sakka and P. Loboda, *J. Alloys Compd.*, 485, 677–681 (2009).
3) I. Bogomol, P. Badica, Y. Shen, T. Nishimura, P. Loboda and O. Vasylkiv, *J. Alloys Compd.*, 570, 94–99 (2013).
4) R. M. White and E. C. Dickey, *J. Am. Ceram. Soc.*, 94, 4032–4039 (2011).
5) O. N. Grigor'ev, V. V. Koval'chuk, O. I. Zaparozhets, N. D. Bega, B. A. Galanov, E. V. Prilutskii, V. A. Kotenko, T. N. Kutran' and N. A. Dordienko, *Metall Met. Ceram.*, 45, 47–57 (2006).
6) S. S. Ordan'yan, A. I. Dmitriev, K. T. Bizhev and E. K. Stepanenko, *Sov. Powder Metall Met.Ceram.*, 26, 834–836 (1987).
7) V. Skorokhod, Jr. and V. D. Krstic, *J. Mater. Sci. Lett.*, 19, 237–239 (2000).
8) L. S. Sigl and H.-J. Kleebe, *J. Am. Ceram. Soc.*, 78, 2374–2380 (1995).
9) S. Otani, *J. Ceram. Soc. Japan*, 108, 955–956 (2000).
10) T. Mizutani and A. Tsuge, *J. Ceram. Soc. Japan*, 100, 991–997 (1992).
11) H. Tanaka, N. Hirosaki and T. Nishimura, *J. Ceram. Soc. Japan*, 111, 878–882 (2003).
12) D. Demirskyi and Y. Sakka, *J. Am. Ceram. Soc.*, 97, 2376–2378 (2014).
13) D. Demirskyi and Y. Sakka, *J. Ceram. Soc. Japan*, 123, 33–37 (2015).
14) S. Grasso, Y. Sakka and G. Maizza, *Sci. Technol. Adv. Mater.*, 10, 053001 (2009).
15) R. Orru, R. Licheri, A. M. Locci, A. Cincotti and G. Cao, *Mater. Sci. Eng., R*, 63, 127–287 (2009).
16) O. Vasylkiv, H. Borodianska, P. Badica, S. Grasso, Y. Sakka, A. Tok, L. Su, M. Bosman and J. Ma, *J. Nanosci. Nanotechnol.*, 12, 959–965 (2012).
17) H. Borodianska, T. Ludvinskaya, Y. Sakka, I. Uvarova and O. Vasylkiv, *Scr. Mater.*, 61, 1020–1023 (2009).
18) D. Demirskyi and Y. Sakka, *J. Eur. Ceram. Soc.*, 35, 405–410 (2015).
19) B. R. Lawn and E. R. Fuller, *J. Mater. Sci.*, 10, 2016–2024 (1975).
20) K. Tanaka, *J. Mater. Sci.*, 22, 1501–1508 (1987).
21) R. M. White and E. C. Dickey, *J. Eur. Ceram. Soc.*, 34, 2043–2050 (2014).
22) J. Watts, G. E. Hilmas, W. G. Fahrenholtz, D. Brown and B. Clausen, *J. Eur. Ceram. Soc.*, 31, 1811–1820 (2011).
23) M. Taya, S. Hayashi, A. S. Kobayashi and H. S. Yoon, *J. Am. Ceram. Soc.*, 73, 1382–1391 (1990).
24) L. Silvestroni, L. Pienti, S. Guicciardi and D. Sciti, *Compos., Part B Eng.*, 72, 10–20 (2015).
25) S. Grasso, C. Hu, O. Vasylkiv, T. S. Suzuki, S. Guo, T. Nishimura and Y. Sakka, *Scr. Mater.*, 64, 256–259 (2011).
26) P. Badica, H. Borodianska, S. Xie, T. Zhao, D. Demirskyi, P. Li, A. I. Y. Tok, Y. Sakka and O. Vasylkiv, *Ceram. Int.*, 40, 3053–3061 (2014).
27) G. V. Samsonov and I. M. Vinitskii, "Handbook of Refractory Compounds", IFI/Plenum, New York (1980) Chap. 5, p. 293.